ON THE PERFORMANCE OF MOBILE TERMINAL TRACKING IN URBAN GSM NETWORKS USING PARTICLE FILTERS

Carsten Fritsche and Anja Klein

Communications Engineering Lab, Technische Universität Darmstadt
Merckstr. 25, 64283 Darmstadt, Germany
email: {c.fritsche, a.klein}@nt.tu-darmstadt.de

ABSTRACT

A particle filter (PF) and a Rao-Blackwellized particle filter (RBPF) are proposed for mobile terminal tracking in the Global System for Mobile Communication (GSM) network based on received signal level and timing advance measurements. The proposed PF and RBPF are able to cope with errors due to non-line-of-sight propagation, which are modelled as non-Gaussian disturbances. The proposed algorithms have been tested on synthetic and "real world" GSM measurements, and their enhanced performance compared to an extended Kalman filter is shown.

1. INTRODUCTION

In recent years, radio network-based localization methods that provide accurate mobile terminal (MT) location estimates have become an important field for researchers and engineers. On the one hand, this is due to emerging commercial applications such as location sensitive billing, fraud detection or intelligent transportation systems that rely on accurate MT location estimates. On the other hand, the United States Federal Communications Commission (FCC) standard requires all wireless providers to report the location of all E-911 callers within a specified accuracy [1].

Until now, several localization methods have been proposed to solve the problem of locating an MT (an overview can be found, e.g., in [1, 2]). Cellular radio network-based localization methods use, e.g., the received signal strength (RSS), angle of arrival (AoA), round trip time (RTT) or time (difference) of arrival (T(D)oA) measurements, in order to estimate the MT location. The radio signals, however, are usually not designed for localization purposes, so that it is difficult to obtain MT location estimates that rely on a single type of measurement. Furthermore, especially in urban scenarios, multiple reflections at buildings and other obstacles prevent the radio signal from arriving via the direct path. The resulting error due to non-line-of-sight propagation (NLOS) can severely affect the accuracy of the MT location estimates. Thus, methods that efficiently combine different types of measurements and take into account errors due to NLOS propagation are needed.

In [3], an extended Kalman filter (EKF) that combines timing advance (TA) and RSS measurements from the Global System for Mobile Communication (GSM) is proposed which does not take into account errors due to NLOS propagation. In [4], particle filters (PFs) for localization in wireless networks are proposed that are either based on RSS or ToA measurements. Although the effect of NLOS propagation is investigated by means of simulations, the combination of RSS and ToA measurements is not considered. A PF and a Rao-Blackwellized PF (RBPF) for mobility tracking in cellular networks based on RSS measurements is presented in [5]. A Rao-Blackwellized variable rate PF that combines line-of-sight (LOS) signals from satellite, cellular radio and sensor networks, in order to simultaneously determine the MT location and the locations of the sensor nodes is described in [6]. In [7], the interacting multiple model algorithm based on ToA measurements and taking into account NLOS error statistics is investigated. A jump Markov particle filter for mixed LOS/NLOS conditions based on RSS and ToA measurements for indoor scenarios is presented in [8].

This paper is focussed on MT tracking using received signal level (RXLEV) and TA measurements from GSM, as they can be easily obtained from off-the-shelf mobile handsets. A PF and a RBPF is proposed that efficiently can deal with the nonlinear relationship between the measurements and the MT location and the errors due to NLOS propagation, which are modelled as non-Gaussian disturbances. The two algorithms have been tested on synthetic and "real world" GSM measurements, and their enhanced performance with respect to the EKF is demonstrated.

The rest of this paper is organized as follows: In Section II, the MT tracking problem is stated and the corresponding MT motion model and the models for the RXLEV and TA measurements are described. In Section III, the PF and RBPF for the MT tracking problem are introduced. In Section IV and V, the performance of the PF and RBPF is compared to the EKF by means of simulations and experimental results. Section VI concludes the work.

2. PROBLEM STATEMENT

2.1 Motion Model

The objective of MT tracking in cellular radio networks is to recursively estimate the MT kinematic state from a set of measurements. It is assumed that the measurements are available at discrete time steps $k \cdot T_s$, with $k \in \mathbb{N}$, where T_s denotes the sampling time and $\mathbb{N}$ is the set of natural numbers. For the MT tracking problem, the states to be estimated are assumed to be the two-dimensional location and velocity of the MT, i.e., $\mathbf{x} = [x_{\mathrm{MT}}, y_{\mathrm{MT}}, \dot{x}_{\mathrm{MT}}, \dot{y}_{\mathrm{MT}}]^{\mathsf{T}}$. The MT state dynamics are described by a nearly constant velocity model [1], given by

$$\mathbf{x}(k+1) = \mathbf{A}\mathbf{x}(k) + \mathbf{B}\mathbf{v}(k), \tag{1}$$

where $\mathbf{A} = \begin{bmatrix} \mathbf{I}_2 & T_s \cdot \mathbf{I}_2 \\ 0 & \mathbf{I}_2 \end{bmatrix}$, $\mathbf{B} = \begin{bmatrix} T_s^2/2 \cdot \mathbf{I}_2 \\ T_s \cdot \mathbf{I}_2 \end{bmatrix}$, $\mathbf{I}_2$ is the identity matrix of size 2 and $\mathbf{v} = [v_x, v_y]^{\mathsf{T}}$ denotes zero-mean Gaussian process noise with covariance matrix $\mathbf{Q} = \mathrm{diag}(\sigma_x^2, \sigma_y^2)$, where σ_x^2 and σ_y^2 are the noise variances in the x- and y-direction, respectively. In the following, the models

for the RXLEV and TA measurements are introduced.

2.2 Measurement Model

In GSM, the TA is a parameter that is used to maintain frame alignment in the GSM system [9]. Basically, the TA is the round trip time, i.e., the time the radio signal needs to travel from the base station (BS) to the MT and back, quantized to finite precision. Let z_{TA} denote the TA measurement multiplied by $c_0/2$, where c_0 denotes the speed of light. Then, the TA measurement can be modelled as

$$z_{\text{TA}}(k) = h_{\text{TA}}(\mathbf{x}(k)) + w_{\text{TA}}(k), \tag{2}$$

where $h_{\text{TA}}(\mathbf{x}(k)) = d^{(n)}(\mathbf{x}(k))$ denotes the Euclidean distance between the MT and the n-th BS. The random variable $w_{\text{TA}}(k)$ accounts for errors due to quantization, changing propagation conditions - LOS or NLOS situation - and inaccuracies in the measurement equipment.

The TA error is modelled with a two-component Gaussian mixture probability density function (pdf) $p_{\text{TA}}(w_{\text{TA}}(k)) = p_{\text{LOS}} \cdot \mathcal{N}(w_{\text{TA}}(k); \mu_{\text{LOS}}, \sigma^2_{\text{LOS}}) + (1 - p_{\text{LOS}}) \cdot \mathcal{N}(w_{\text{TA}}(k); \mu_{\text{NLOS}}, \sigma^2_{\text{NLOS}})$ [1], where the error $w_{\text{TA}}(k)$ falls in the LOS distribution with probability p_{LOS}, and in the NLOS distribution with probability $(1 - p_{\text{LOS}})$, and where $\mathcal{N}(w_{\text{TA}}(k); \mu, \sigma^2)$ denotes a Gaussian density with mean μ and variance σ^2. This assumption can be verified by experimental data, cf. Fig. 1, that have been obtained from field trials in an urban city center in Germany. From Fig. 1, it is obvious that compared to the Gaussian mixture pdf, the single Gaussian pdf only poorly approximates the true TA error pdf.

Unfortunately, off-the-shelf mobile phones only receive the TA from the serving BS, which is not enough information to uniquely determine the MT location. In GSM, however, additional MT location information can be obtained from the RXLEV measurements, which are quantized RSS measurements. In general, the MT measures the RSS from up to $N_{\text{BS}} = 7$ BSs. Let $\mathbf{z}_{\text{RSS}}(k)$ denote the vector of N_{BS} RSS measurements. Then, the model for the RSS measurement in dB scale is given by

$$\mathbf{z}_{\text{RSS}}(k) = \mathbf{h}_{\text{RSS}}(\mathbf{x}(k)) + \mathbf{w}_{\text{RSS}}(k) \tag{3}$$

[1], with $\mathbf{h}_{\text{RSS}}(\mathbf{x}(k)) = [h^{(1)}_{\text{RSS}}(\mathbf{x}(k)), \cdots, h^{(N_{\text{BS}})}_{\text{RSS}}(\mathbf{x}(k))]^{\mathsf{T}}$, where $h^{(n)}_{\text{RSS}}(\mathbf{x}(k)) = P^{(n)}_{\text{t}} - L^{(n)}(\mathbf{x}(k))$, $P^{(n)}_{\text{t}}$ denotes the equivalent isotropic radiated power of the n-th BS and $L^{(n)}(\mathbf{x}(k))$ is the path loss. The path loss is given by the well known formula

$$L^{(n)}(\mathbf{x}(k)) = A^{(n)} + 10 \cdot B^{(n)} \cdot \log_{10}\left(d^{(n)}(\mathbf{x}(k))/\text{km}\right),$$

where $A^{(n)}$ and $B^{(n)}$ are model parameters that strongly depend on the BS antenna settings and the investigated scenario. The random variable $\mathbf{w}_{\text{RSS}}(k)$ accounts for errors, such as, quantization errors and errors due to slow fading and NLOS propagation, which can be assumed to be zero-mean Gaussian distributed with multivariate pdf $p_{\text{RSS}}(\mathbf{w}_{\text{RSS}}(k)) = \mathcal{N}(\mathbf{w}_{\text{RSS}}(k); \mathbf{0}, \mathbf{R}_{\text{RSS}})$ and covariance matrix $\mathbf{R}_{\text{RSS}}$. It is assumed that the covariance matrix is given by $\mathbf{R}_{\text{RSS}} = \text{diag}((\sigma^{(1)}_{\text{RSS}})^2, \cdots, (\sigma^{(N_{\text{BS}})}_{\text{RSS}})^2)$. Note that the errors due to NLOS are implicitly included in the model [10].

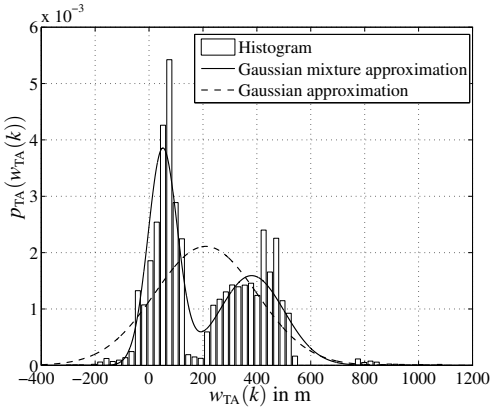

Figure 1: Empirical TA error pdf from outdoor field trial and corresponding Gaussian and Gaussian mixture approximations.

3. PARTICLE FILTERS FOR MOBILE TERMINAL TRACKING

3.1 Recursive Bayesian Estimation

After having described the TA and RSS measurements that are corrupted by (non-)Gaussian noise and that are nonlinearly related to the MT location, the question is how one can efficiently recursively estimate the MT location from these measurements. Let $\mathbf{Z}(k) = \{\mathbf{z}(l), l = 1, ..., k\}$ denote the sequence of available measurements up to time k, with $\mathbf{z}(l) = [z_{\text{TA}}(l), \mathbf{z}^{\mathsf{T}}_{\text{RSS}}(l)]^{\mathsf{T}}$. Then, from a Bayesian point of view, the solution to the above problem is to recursively compute the posterior pdf $p(\mathbf{x}(k)|\mathbf{Z}(k))$ of the MT state vector, given the data $\mathbf{Z}(k)$. The optimal Bayesian solution, provided that certain assumptions hold, is given by the following two recurrence relations

$$p(\mathbf{x}(k)|\mathbf{Z}(k)) = \frac{p(\mathbf{z}(k)|\mathbf{x}(k))p(\mathbf{x}(k)|\mathbf{Z}(k-1))}{p(\mathbf{z}(k)|\mathbf{Z}(k-1))},$$

$$p(\mathbf{x}(k+1)|\mathbf{Z}(k)) = \int p(\mathbf{x}(k+1)|\mathbf{x}(k))p(\mathbf{x}(k)|\mathbf{Z}(k))\text{d}\mathbf{x}(k)$$

[11, 12], where $p(\mathbf{z}(k)|\mathbf{Z}(k-1))$ is a normalizing constant, and where the pdfs $p(\mathbf{x}(k+1)|\mathbf{x}(k))$ and $p(\mathbf{z}(k)|\mathbf{x}(k))$ can be determined from (1) and (2), (3), respectively. However, due to the nonlinear and (non-)Gaussian structure of the measurement model, cf. (2) and (3), an analytical solution of the above recursions is intractable. Thus, in order to solve the underlying MT tracking problem, one has to resort to suboptimal algorithms.

3.2 Particle Filter

The MT tracking problem is solved using sequential Monte Carlo methods that are commonly referred to as particle filters [11–14]. The PF is based on a recursive approximation of the posterior pdf $p(\mathbf{x}(k)|\mathbf{Z}(k))$ by a set of N random samples $\mathbf{x}_i(k)$ (particles) with corresponding importance weights $w_i(k)$, i.e.,

$$p(\mathbf{x}(k)|\mathbf{Z}(k)) \approx \sum_{i=1}^{N} w_i(k) \cdot \delta(\mathbf{x}(k) - \mathbf{x}_i(k)),$$

where $\delta(\cdot)$ denotes the Dirac delta function. In Table 1, the PF for the MT tracking problem is presented that uses the

Table 1: Particle Filter for MT Tracking

1. Initialization ($i = 1, ..., N$)
   Generate samples and initialize weights:
   $\mathbf{x}_i(0) \sim p(\mathbf{x}(0)), \quad w_i(0) = 1/N$
   where "$\sim$" means "is distributed according to" and $p(\mathbf{x}(0))$ is the prior distribution of the MT state vector at $k = 0$.
2. Measurement update ($i = 1, ..., N$)
   Update the weights and normalize:
   $$w_i(k) = \frac{p(\mathbf{z}(k)|\mathbf{x}_i(k))w_i(k-1)}{\sum_{j=1}^{N} p(\mathbf{z}(k)|\mathbf{x}_j(k))w_j(k-1)}$$
3. Effective sample size N_{eff} and PF output calculation
   $N_{\text{eff}} = 1/\sum_{i=1}^{N}(w_i(k))^2, \quad \hat{\mathbf{x}}(k) = \sum_{i=1}^{N} w_i(k)\mathbf{x}_i(k)$
4. Resampling with replacement
   Only resample when $N_{\text{eff}} < N_{\text{th}}$. Then, take N samples $\mathbf{x}_i(k)$ with replacement from the old set $\{\mathbf{x}_j(k), j = 1, ..., N\}$, where $\Pr\{\mathbf{x}_i(k) = \mathbf{x}_j(k)\} = w_j(k)$. Set $w_i(k) = 1/N$, for $i = 1, ..., N$.
5. Prediction ($i = 1, ..., N$)
   Predict the samples:
   $\mathbf{x}_i(k+1) \sim \mathcal{N}(\mathbf{x}_i(k+1); \mathbf{A}\mathbf{x}_i(k), \mathbf{B}\mathbf{Q}\mathbf{B}^{\mathsf{T}})$

transitional prior as an importance density function. The PF algorithm consists of three major steps: measurement update, resampling and prediction [13].

Step 1: Measurement update. Upon the arrival of a new measurement, the importance weight $w_i(k)$ of each particle $\mathbf{x}_i(k)$ is updated via the likelihood function $p(\mathbf{z}(k)|\mathbf{x}(k))$.

Step 2: Resampling. In the resampling step, particles $\mathbf{x}_i(k)$ with low importance weights $w_i(k)$ are eliminated and particles with high importance weights are multiplied, in order to avoid a poor approximation of the posterior pdf $p(\mathbf{x}(k)|\mathbf{Z}(k))$.

Step 3: Prediction. In the prediction step, the predicted particles $\mathbf{x}_i(k+1)$ are sampled from the transitional density $p(\mathbf{x}(k+1)|\mathbf{x}(k))$ in order to approximate $p(\mathbf{x}(k+1)|\mathbf{Z}(k))$.

3.3 Rao-Blackwellized Particle Filter

It is well known that the computational complexity of the PF becomes prohibitively high when a large number of particles is used. In order to overcome this problem, a technique called Rao-Blackwellization can be applied to PFs (a comprehensive treatment of RBPFs can be found, e.g., in [14–18]).

The main idea behind Rao-Blackwellization is to partition the state vector $\mathbf{x}(k) = [\mathbf{x}^{\text{kf}}(k), \mathbf{x}^{\text{pf}}(k)]^{\mathsf{T}}$ into linear states $\mathbf{x}^{\text{kf}}(k)$ and nonlinear states $\mathbf{x}^{\text{pf}}(k)$ and then to analytically marginalize out the linear states from the resulting joint posterior pdf $p(\mathbf{x}^{\text{kf}}(k), \mathbf{x}^{\text{pf}}(k)|\mathbf{Z}(k))$ [16]. It can be shown that the linear states can then be estimated by a Kalman filter, and the nonlinear states can be estimated by a PF. The result of this technique is that, compared to a standard PF, the variance of the state estimates can be reduced.

For the MT tracking problem, the MT velocity components are estimated with the Kalman filter, i.e., $\mathbf{x}^{\text{kf}} = [\dot{x}_{\text{MT}}, \dot{y}_{\text{MT}}]^{\mathsf{T}}$, and the MT location is estimated with the particle filter, i.e., $\mathbf{x}^{\text{pf}} = [x_{\text{MT}}, y_{\text{MT}}]^{\mathsf{T}}$. Thus, the motion and measurement model, cf. (1), (2) and (3), can be rewritten as

$$\begin{pmatrix}\mathbf{x}^{\text{pf}}(k+1)\\ \mathbf{x}^{\text{kf}}(k+1)\end{pmatrix} = \begin{pmatrix}\mathbf{I}_2 & \mathbf{A}^{\text{pf}}\\ \mathbf{0} & \mathbf{A}^{\text{kf}}\end{pmatrix}\begin{pmatrix}\mathbf{x}^{\text{pf}}(k)\\ \mathbf{x}^{\text{kf}}(k)\end{pmatrix} + \begin{pmatrix}\mathbf{B}^{\text{pf}}\\ \mathbf{B}^{\text{kf}}\end{pmatrix}\mathbf{v}(k), \quad (4)$$

$$\mathbf{z}(k) = \mathbf{h}(\mathbf{x}^{\text{pf}}(k)) + \mathbf{w}(k), \quad (5)$$

where $\mathbf{A}^{\text{pf}} = T_{\text{s}} \cdot \mathbf{I}_2$, $\mathbf{A}^{\text{kf}} = \mathbf{I}_2$, $\mathbf{B}^{\text{pf}} = T_{\text{s}}^2/2 \cdot \mathbf{I}_2$ and $\mathbf{B}^{\text{kf}} = T_{\text{s}} \cdot \mathbf{I}_2$. The process noise $\mathbf{v} = [\mathbf{v}^{\text{pf}}, \mathbf{v}^{\text{kf}}]^{\mathsf{T}}$ is zero-mean Gaussian distributed with covariance matrix $\tilde{\mathbf{Q}} = \mathbf{1}_2 \otimes \mathbf{Q}$, where $\otimes$ is the Kronecker product and $\mathbf{1}_2$ denotes a matrix of size 2 whose entries are all 1. The RBPF for the underlying MT tracking problem is given in Table 2.

4. SIMULATION SCENARIO AND RESULTS

For the simulations, it is assumed that a car travels with a constant speed of 70 km/h on a straight line, starting at (0 km, 0 km) and ending at approximately (1.3 km, 1.3 km). The car is equipped with an MT that provides RXLEV and TA measurements from the GSM network. The GSM network is composed of $N_{\text{BS}} = 7$ BSs with known BS locations, where each BS is equipped with a single omni-directional antenna. The BS locations are given by (-0.75 km, 0.75 km), (-0.25 km, 1.5 km), (0.75 km, 1.75 km), (0.5 km, -0.75 km), (1.5 km, 0 km), (2 km, 1.9 km) and (-0.75 km, -0.6 km). It is assumed that the MT receives one TA from the serving BS and a total of seven RXLEV measurements from the serving

Table 2: Rao-Blackwellized Particle Filter for MT Tracking

1. Initialization of Kalman and Particle filters ($i = 1, ..., N$)
   $\hat{\mathbf{x}}_i^{\text{kf}}(0|-1) \sim p(\hat{\mathbf{x}}^{\text{kf}}(0|-1)), \ \mathbf{x}_i^{\text{pf}}(0) \sim p(\mathbf{x}^{\text{pf}}(0)), \ w_i(0) = 1/N$
2. Particle filter measurement update ($i = 1, ..., N$)
   $$w_i(k) = \frac{p(\mathbf{z}(k)|\mathbf{x}_i^{\text{pf}}(k))w_i(k-1)}{\sum_{j=1}^{N} p(\mathbf{z}(k)|\mathbf{x}_j^{\text{pf}}(k))w_j(k-1)}$$
3. Effective sample size N_{eff} and PF output calculation
   $N_{\text{eff}} = 1/\sum_{i=1}^{N}(w_i(k))^2, \quad \hat{\mathbf{x}}^{\text{pf}}(k) = \sum_{i=1}^{N} w_i(k)\mathbf{x}_i^{\text{pf}}(k)$
4. Resampling with replacement (see Table 1)
5. Particle filter prediction ($i = 1, ..., N$)
   $$\mathbf{x}_i^{\text{pf}}(k+1) \sim \mathcal{N}(\mathbf{x}_i^{\text{pf}}(k+1); \mathbf{x}_i^{\text{pf}}(k) + \mathbf{A}^{\text{pf}}\hat{\mathbf{x}}_i^{\text{kf}}(k|k-1), \mathbf{A}^{\text{pf}}\mathbf{P}^{\text{kf}}(k|k-1)(\mathbf{A}^{\text{pf}})^{\mathsf{T}} + \mathbf{B}^{\text{pf}}\mathbf{Q}(\mathbf{B}^{\text{pf}})^{\mathsf{T}})$$
6. Measurement update of the Kalman filters ($i = 1, ..., N$)
   $$\tilde{\mathbf{z}}_i(k) = \mathbf{x}_i^{\text{pf}}(k+1) - \mathbf{x}_i^{\text{pf}}(k)$$
   $$\mathbf{S}(k) = \mathbf{A}^{\text{pf}}\mathbf{P}^{\text{kf}}(k|k-1)(\mathbf{A}^{\text{pf}})^{\mathsf{T}} + \mathbf{B}^{\text{pf}}\mathbf{Q}(\mathbf{B}^{\text{pf}})^{\mathsf{T}}$$
   $$\mathbf{K}(k) = \mathbf{P}^{\text{kf}}(k|k-1)(\mathbf{A}^{\text{pf}})^{\mathsf{T}}(\mathbf{S}(k))^{-1}$$
   $$\hat{\mathbf{x}}_i^{\text{kf}}(k|k) = \hat{\mathbf{x}}_i^{\text{kf}}(k|k-1) + \mathbf{K}(k)(\tilde{\mathbf{z}}_i(k) - \mathbf{A}^{\text{pf}}\hat{\mathbf{x}}_i^{\text{kf}}(k|k-1))$$
   $$\mathbf{P}^{\text{kf}}(k|k) = \mathbf{P}^{\text{kf}}(k|k-1) - \mathbf{K}(k)\mathbf{A}^{\text{kf}}\mathbf{P}^{\text{kf}}(k|k-1)$$
7. Prediction of the Kalman filters ($i = 1, ..., N$)
   $$\mathbf{C} = \mathbf{A}^{\text{kf}} - \mathbf{B}^{\text{kf}}(\mathbf{B}^{\text{pf}})^{-1}\mathbf{A}^{\text{pf}}$$
   $$\hat{\mathbf{x}}_i^{\text{kf}}(k+1|k) = \mathbf{C}\hat{\mathbf{x}}_i^{\text{kf}}(k|k) + \mathbf{B}^{\text{kf}}(\mathbf{B}^{\text{pf}})^{-1}\tilde{\mathbf{z}}_i(k)$$
   $$\mathbf{P}^{\text{kf}}(k+1|k) = \mathbf{C}\mathbf{P}^{\text{kf}}(k|k)\mathbf{C}^{\mathsf{T}}$$

and neighboring BS antennas. The serving BS is assumed to be the BS providing the largest RXLEV.

The simulation parameters are given in Table 3 and are assumed to be equal for all BSs for the sake of simplicity. Note that the error pdf for the TA measurement is modelled as a two-component Gaussian mixture. The unknown parameters of the Gaussian mixture have been estimated from the field trial data, cf. Fig. 1, using the Expectation Maximization algorithm. The accuracy of the proposed PF and RBPF algorithms is evaluated in terms of the position root mean square error (RMSE) determined from $N_{\mathrm{MC}} = 100$ Monte Carlo trials. The threshold for resampling is chosen as $N_{\mathrm{th}} = 2N/3$. For comparison, simulations have been carried out for an EKF that approximates the error pdf of the TA measurement, cf. Fig. 1, with a single Gaussian density with mean $\mu_{\mathrm{EKF}} = 210\,\mathrm{m}$ and standard deviation $\sigma_{\mathrm{EKF}} = 190\,\mathrm{m}$.

Table 3: Simulation parameters

Parameter	Value	Parameter	Value
A in dB	132.8	T_{s} in s	0.48
B in dB	3.8	p_{LOS}	0.52
σ_{RSS} in dB	6	μ_{LOS} in m	51
P_{t} in dBm	33	σ_{LOS} in m	55
σ_x in m/s^2	1	μ_{NLOS} in m	380
σ_y in m/s^2	1	σ_{NLOS} in m	120

In Fig. 2, the RMSE in dependence of the time index k for the EKF, PF and RBPF using $N = 250$ and $N = 1000$ particles is shown. Compared to the PF and RBPF, the EKF provides the worst results in terms of RMSE. On the one hand, this is due to the fact that the EKF has to linearize the nonlinear measurement equations, which results in a degradation of the performance. On the other hand, the EKF only poorly approximates the non-Gaussian TA error pdf which further results in performance loss. The PF and RBPF, however, can efficiently deal with the nonlinear measurement model and non-Gaussian error which results in performance improvement, but they have the disadvantage of being computationally more complex. For a small number of particles and thus, a lower computational complexity, the RBPF gives more accurate results than the PF.

Even though the details of the algorithms are not presented in this paper, simulations have been carried out using the auxiliary particle filter (AUX-PF) and regularized particle filter with Epanechnikov kernel (RPF-EPA) and Gaussian kernel (RPF-GAU) [11–13]. The results on the position RMSE averaged over the whole time period for different numbers of

Table 4: Average RMSE in m for the different algorithms

Algorithm	Number of Particles			
	250	500	1000	2000
PF	50.8	43.1	42.2	41.2
RBPF	46.8	43.1	42.1	41.4
AUX-PF	50.1	45.2	42.3	41.5
RPF-GAU	55.4	51.9	49.3	47.4
RPF-EPA	47.7	46.4	45.3	44.5
EKF	64.1			

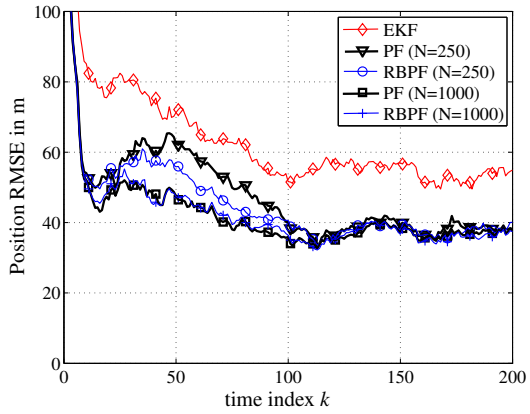

Figure 2: Position RMSE for the EKF, PF and RBPF ($N = 250, 1000$ particles) and $N_{\mathrm{MC}} = 100$.

particles and for $N_{\mathrm{MC}} = 100$ Monte Carlo runs are summarized in Table 4. From Table 4 it can be seen that in terms of average RMSE and for a small number of particles, the RBPF provides the best results compared to the other PFs.

5. EXPERIMENTAL RESULTS

In this section, the proposed PF and RBPF are tested on GSM measurements available from a field trial. The field trial was conducted in an operating GSM network in a German city center, where the test area has a size of approximately $3\,\mathrm{km} \times 3\,\mathrm{km}$. During the field trial every $T_{\mathrm{s}} = 0.48\,\mathrm{s}$, a car equipped with a standard cellular phone collected RXLEV and TA measurements from GSM. Note that in GSM the RXLEV measurements are available from the serving BS and between one and six strongest RXLEVs from the neighboring BSs, whereas the TA measurement is only available from the serving BS. The investigated GSM network is composed of $N_{\mathrm{BS}} = 13$ fixed BSs with known locations. The BSs are either equipped with omni-directional or directional antennas.

In Fig. 3, the true MT trajectory and the trajectories estimated from the EKF, PF and RBPF for $N = 1000$ particles

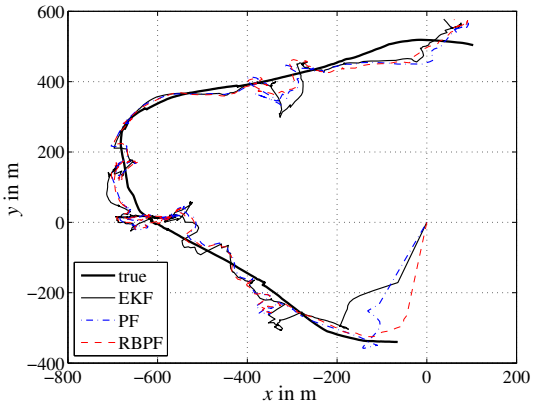

Figure 3: Field trial scenario with true MT trajectory and estimated trajectories from the EKF, PF and RBPF ($N = 1000$ particles).

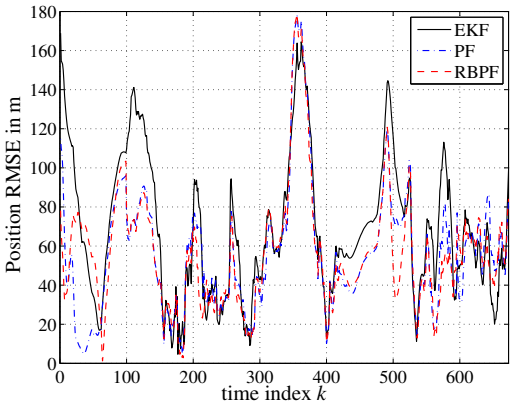

Figure 4: Position RMSE for the EKF, PF and RBPF ($N = 1000$ particles) based on field trial data.

are shown. The true MT location was obtained from detailed maps and GPS, where GPS was available. Speed constraints are additionally included in the PF and RBPF in order to improve the performance [5]. From Fig. 3 it can be clearly seen that all three algorithms can track the MT. In Fig. 4, the postion RMSE is depicted for the three algorithms. It can be seen that the EKF provides the worst performance. The accuracy can be further improved by the PF and RBPF, where the RBPF provides approximately the same accuracy as the PF. The peaks in the position RMSE can be explained by the bad geometric constellation of the BSs relative to the MT and the change of MT velocity during the field trial.

6. CONCLUSION

In this paper, a particle filter and a Rao-Blackwellized particle filter are proposed that combine RXLEV and TA measurements from the GSM network, in order to accurately track the MT. The achievable accuracy of the filters is compared to the EKF technique and their enhanced performance is shown based on synthetic and field trial data. In a next step, for instance the performance of the proposed PF and RBPF could be improved by considering importance density functions that better approximate the optimal importance density. Furthermore, for the special case of non-Gaussian measurement noise, the theoretical performance could be assessed by evaluating the posterior Cramér-Rao bound.

REFERENCES

[1] F. Gustafsson and F. Gunnarsson, "Mobile positioning using wireless networks," *IEEE Signal Processing Mag.*, vol. 22, no. 4, pp. 41–53, Jul. 2005.

[2] A. H. Sayed, A. Tarighat, and N. Khajehnouri, "Network-based wireless location: challenges faced in developing techniques for accurate wireless location information," *IEEE Signal Processing Mag.*, vol. 22, no. 4, pp. 24–40, Jul. 2005.

[3] M. Zhang, S. Knedlik, P. Ubolkosold, and O. Loffeld, "A data fusion approach for improved positioning in GSM networks," in *Proc. IEEE/ION Position, Location, and Navigation Symposium*, San Diego, USA, Apr. 2006, pp. 218–222.

[4] P.-J. Nordlund, F. Gunnarsson, and F. Gustafsson, "Particle filters for positioning in wireless networks," in *Proc. European Signal Processing Conference*, vol. 2, Toulouse, France, Sept. 2002, pp. 311–314.

[5] L. Mihaylova, D. Angelova, S. Honary, D. Bull, C. N. Canagarajah, and B. Ristic, "Mobility tracking in cellular networks using particle filtering," *IEEE Trans. Wireless Commun.*, vol. 6, pp. 3589–3599, Oct. 2007.

[6] C. Fernández-Prades, P. Closas, and J. A. Fernández-Rubio, "Rao-Blackwellized variable rate particle filtering for handset tracking in communication and sensor networks," in *Proc. European Signal Processing Conference*, Poznań, Poland, Sept. 2007, pp. 111–115.

[7] C. Fritsche, U. Hammes, A. Klein, and A. Zoubir, "Robust mobile terminal tracking in NLOS environments using interacting multiple model algorithm," in *Proc. IEEE Int. Conf. Acoust., Speech, Signal Process.*, Taipei, Taiwan, Apr. 2009.

[8] M. Nicoli, C. Morelli, and V. Rampa, "A jump markov particle filter for localization of moving terminals in multipath indoor scenarios," *IEEE Trans. Signal Processing*, vol. 56, no. 8, pp. 3801–3809, Aug. 2008.

[9] A. Küpper, *Location-based services*, 1st ed. John Wiley & Sons, 2005.

[10] Y. Qi, H. Kobayashi, and H. Suda, "Analysis of wireless geolocation in a non-line-of-sight environment," *IEEE Trans. Wireless Commun.*, vol. 5, no. 3, pp. 672–681, Mar. 2006.

[11] B. Ristic, S. Arulampalam, and N. Gordon, *Beyond the Kalman Filter: Particle Filters for Tracking Applications*. Artech-House, 2004.

[12] A. Doucet, N. de Freitas, and N. Gordon, *Sequential Monte Carlo Methods in Practice*. Springer-Verlag, 2001.

[13] M. S. Arulampalam, S. Maskell, N. Gordon, and T. Clapp, "A tutorial on particle filters for online nonlinear/non-Gaussian Bayesian tracking," *IEEE Trans. Signal Processing*, vol. 50, no. 2, pp. 174–188, Feb. 2002.

[14] F. Gustafsson, F. Gunnarsson, N. Bergman, U. Forssell, J. Jansson, R. Karlsson, and P. Nordlund, "Particle filters for positioning, navigation and tracking," *IEEE Trans. Signal Processing*, vol. 50, no. 2, pp. 425–437, Feb. 2002.

[15] C. Andrieu and A. Doucet, "Particle filtering for partially observed Gaussian state space models," *J. R. Statist. Soc.*, vol. 64, no. 4, pp. 827–836, 2002.

[16] T. Schön, F. Gustafsson, and P.-J. Nordlund, "Marginalized particle filters for mixed linear/nonlinear state-space models," *IEEE Trans. Signal Processing*, vol. 53, no. 7, pp. 2279–2289, Jul. 2005.

[17] P.-J. Nordlund and F. Gustafsson, "Sequential Monte Carlo techniques applied to integrated navigation systems," in *Proc. American Control Conference*, Arlington, Virginia, USA, Jun. 2001, pp. 4375–4380.

[18] R. Karlsson, T. Schön, and F. Gustafsson, "Complexity analysis of the marginalized particle filter," *IEEE Trans. Signal Processing*, vol. 53, no. 11, pp. 4408–4411, Nov. 2005.